



# Synthesis and Characterization of Silicon Nitride Reinforced Al–Mg–Zn Alloy Composites

G. Anbuechhiyan<sup>1</sup> · B. Mohan<sup>2</sup> · N. Senthilkumar<sup>3</sup> · R. Pugazhenti<sup>4</sup>

Received: 2 September 2020 / Accepted: 22 October 2020  
© The Korean Institute of Metals and Materials 2021

## Abstract

In this work, aluminium metal matrix composite reinforced with hard silicon nitride ( $\text{Si}_3\text{N}_4$ ) particles have been performed experimentally. Squeeze casting technique was adopted to synthesis the novel AMMC for different weight fractions of  $\text{Si}_3\text{N}_4$  (3, 6 and 9%). The AMMC is characterized for their tensile strength, micro-Vickers, density and porosity, compressive strength, impact, corrosion and wear resistance, as per ASTM standards. Observation shows that, with the inclusion of  $\text{Si}_3\text{N}_4$  particle, the mechanical behaviour, corrosion and wear-resistant of synthesized composites was considerably improved. Scanning Electron microscope micrograph of worn surfaces displays the presence of grooves parallel to the sliding direction and some plastic deformations. The inclusion of  $\text{Si}_3\text{N}_4$  shows deep grooving, that is associated with abrasive wear.

**Keywords** Aluminium composite · Squeeze casting · Tensile strength · Pin-on-disc · Porosity · Micro-Vickers

## 1 Introduction

Owing to its low density, high specific strength, stiffness, superior damping capacity, low coefficient of thermal expansion, better corrosion resistant and potential to strengthen using precipitation hardening the development of aluminium

metal matrix composites is mostly used as engineering materials for automobile, aerospace and marine applications. Moreover, the inherence of chemical composition presents in aluminium alloys offer a wide variety of mechanical properties [1, 2]. However, these alloys have low melting points, low modulus of elasticity, inferior hardness, and poor wear resistance. This limits the use of aluminium and its alloy for functional applications. It can be resolved by adding suited hard ceramic reinforcement particulates into the aluminium and its alloy matrix to enhance such properties [3]. The ceramic reinforcements such as  $\text{Al}_2\text{O}_3$ , SiC,  $\text{B}_4\text{C}$ , BN, AlN,  $\text{Ni}_3\text{Al}$ ,  $\text{AlB}_2$  are commonly used as reinforcement to synthesize aluminium alloy composites [4, 5]. It has been there that the exploitation of aluminium and its alloys are used as a matrix material for producing aluminium composites for dissimilar applications [6]. Currently, Al7075 aluminium alloy has been primarily used as matrix materials for automobile and marine applications. Since these materials possess non-uniformity in composition and it results in microsegregation which consequently improves the mechanical properties of manufactured composites. In addition to that these alloys have a reduction in properties such as formability, wear, and corrosion-resistant. But still, there is a scope for increasing its mechanical properties by adding various ceramic reinforcement into it [7]. Silicon nitride ( $\text{Si}_3\text{N}_4$ ) includes of  $\beta$ -particles in an  $\alpha$ -phase, which is consistently utilize to formulate a microstructure incorporation of better elongated

✉ G. Anbuechhiyan  
tsgaaa1981@gmail.com

B. Mohan  
mohan@mitindia.edu

N. Senthilkumar  
nsmkfg@gmail.com

R. Pugazhenti  
pugal4@gmail.com

<sup>1</sup> Department of Mechanical Engineering, SRM Valliammai Engineering College, Kattankulathur, Chennai, Kancheepuram, TamilNadu 603203, India

<sup>2</sup> Department of Mechanical Engineering, CEG Campus, Anna University, Chennai, TamilNadu 600025, India

<sup>3</sup> Department of Mechanical Engineering, Adhiparasakthi Engineering College, Melmaravathur, Kancheepuram, TamilNadu 603319, India

<sup>4</sup> Department of Mechanical Engineering, Vels Institute of Science, Technology and Advanced Studies, Chennai, Kancheepuram, TamilNadu 600117, India

$\beta$ -grains in a matrix of finer  $\beta$ -grains and an inadequate crystallized grain boundary phase. Because of enlarged grains, it exhibits steady-state toughness values, high compressive strength and good wear resistance. The ceramic reinforcement such as  $\text{Al}_2\text{O}_3$ , SiC, BN, etc. is used to enhance the physical properties of aluminium and its alloy under friction and adequate temperature environment for functional applications. However, the nitride strengthening particulates are precisely used to develop aluminium composites for the applications where high heat conductivity, high specific modulus, low density and stability at high temperature is further essential. In comparison with other ceramic particulates, the inclusion of  $\text{Si}_3\text{N}_4$  in base material has various advantageous characteristics such as low thermal expansion, high specific strength, thermal conductivity, and dimensional stability, toughness, thermal shock and oxidation resistance. Considering that it has been used as reinforcement for synthesizing aluminium alloy composites in the present study. Different methods and alloys have been used to synthesis  $\text{Si}_3\text{N}_4$  reinforced aluminium composites and its mechanical properties were characterized. The effect of  $\text{Si}_3\text{N}_4$  on Al 2024 alloys was developed by varying its volume percentage and it was characterized. The bending strength and elastic modulus of composites significantly decreased [8]. The properties of  $\text{Si}_3\text{N}_4$  reinforced AA 6082-T6 aluminium composites were developed using a stir casting method and it was observed that the mechanical properties of synthesized composites increased and the ductility was reduced [9]. The microstructure and mechanical properties of  $\text{Si}_3\text{N}_4$  reinforced Al6061 aluminium composites by varying its volume fraction using the powder metallurgy method have been developed. It was observed that the mechanical properties of synthesized composites significantly decreased due to an increase in the percentage of reinforcement.

From the literature study, it is clearly analysed that only a few research work has been concentrated and characterized by synthesizing  $\text{Si}_3\text{N}_4$  reinforced Al7075 aluminium alloy composites by adding a minimum weight percentage of reinforcement through squeeze casting processing method. In this context, an endeavour has been to synthesize  $\text{Si}_3\text{N}_4$  reinforced Al 7075 aluminium alloy by varying its weight percentage (3%, 6% and 9%) using the squeeze casting method and its mechanical properties have been characterized.

## 2 Experimental Methodology

### 2.1 Selection of Materials

In the present study Al7075 aluminium alloy is used as matrix material and its chemical compositions are shown in Table 1. The commercially available predominantly  $\alpha$  phase of  $\text{Si}_3\text{N}_4$  particle size  $\leq 10$  microns from sigma Aldrich is used as reinforcement for synthesizing aluminium composites. Among various processing methods, squeeze casting has been used for homogenising aluminium composites. In this method, the liquid slurry is fed into the permanent die and pressure is applied consequently by hydraulic ram until the composites get solidified. In addition to that this process is simple, economical and the microstructure refinement of squeeze casting is more advantageous compared to other processing methods [10].

### 2.2 Squeeze Casting Process

In this necessitates quantity of Al7075 alloy is allowed to melt in a resistance heating furnace at 700 °C. To obtain homogenous melt the furnace temperature is increased to 750 °C for 20 min. Due to the existence of magnesium in Al7075 alloy, a mixture of Argon and  $\text{SF}_6$  gas of 3.5 l/min is allowed to enter into the furnace to prevent oxidation and excess burning. In order to enhance the wettability between the base material and ceramic strengthening particulates the  $\text{Si}_3\text{N}_4$  particulates are preheated to 350 °C and then it is allowed to add with a molten alloy. The reinforcement of  $\text{Si}_3\text{N}_4$  of varying weight percentages (3 wt%, 6 wt%, 9 wt%) is added into the molten metal through external sprue. The temperature of the molten metal is increased to 850 °C. To ensure homogeneous distribution of reinforcement in the matrix melt the stirring speed and stirring time have been maintained at 600 rpm and 15 min respectively. Finally, the molten aluminium composites slurry is poured into the preheated die cavity of dimensioned size (120mm\*120mm\*25 mm) and followed by that a pressure of 200 MPa is applied to pressurize the molten composite slurry until the composites get solidified [11, 12] as shown in Fig. 1.

**Table 1** Chemical composition of Al7075

Concentration of wt%								
Cr	Cu	Fe	Mg	Mn	Si	Ti	Zn	Al
0.28	2	0.50	2.6	0.30	0.40	0.20	5.8	Balance



(a) Squeeze casting Setup used for synthesis of Silicon nitride reinforced aluminium composites.



(b) Composites of silicon nitride obtained using squeeze casting by varying its weight percentage (3%, 6% & 9%)

Fig. 1 Experimental setup used for synthesizing  $\text{Si}_3\text{N}_4$  reinforced Al–Mg–Zn alloy composites

### 2.3 Performance Measures of Synthesized Composites

The samples for finding the properties of  $\text{Si}_3\text{N}_4$  reinforced aluminium composites have been prepared as per ASTM standards. Two sets of aluminium composite samples are prepared by varying its weight proportions (3 wt%, 6 wt%, 9 wt%) and it has been characterized. De-winter inverted a trinocular metallurgical microscope is used to investigate the texture of synthesized composites. Keller's reagent solution is used as an etchant. Micro Vickers hardness test has been used to evaluate the microhardness of aluminium composites on a load range 10 g to 1 kg by using Wilson Wolpert

Germany. ASTM E562 & E125 software is used to identify the density and porosity phase and volume analysis of developed composites. In addition to that ASTM standard of E8, E9, E23 is used to characterize the tensile, compressive and impact resistance of synthesized aluminium composite and their composite samples are shown in Fig. 2.

The parameters that are used to measure corrosion tests as per ASTM B117 salt spray test are given in Table 2. Finally, the corrosion samples were cleaned with 10% HCl and 1 g of hexamethylenediamine and heated for some time and were tested.

In the present study, pin-on-disc method is used to study the wear properties of  $\text{Si}_3\text{N}_4$  reinforced aluminium



Fig. 2  $\text{Si}_3\text{N}_4$  reinforced composites prepared and characterized as per ASTM standards

**Table 2** Testing parameters used for evaluating corrosion properties of aluminum composites

S. no	Details of testing parameters	
1	Humidity	98% as measured by hygrometer during the test.
2	Temperature of the test	33 to 35 Degrees centigrade. (Continuously indicated).
3	Pressure of air for atomizing	2 to 3 bar continuously by pressure regulator
4	Composition of the salt solution	For 1 liter of solution. (5% of Sodium chloride, 1% of Magnesium chloride, de-ionized water 94%)
5	PH of the solution	Maintained at 7.5 by addition of buffer solution
6	Measurement of pH	Measured once in 8 h
7	Type of loading of specimens	Tie Tied with plastic wire and hung in the hangers
8	Measurement of Corrosion	The weight of the sample at the time of hanging initially and after 2 h 24 h is measured to know the corrosion amount

composites under dry sliding conditions as per ASTM G99-04. The synthesized composite samples of varying weight percentage are prepared in the form of a 6 mm diameter and 35 mm length. The steel material EN31 of surface roughness  $0.3 \mu\text{m}$  is used as a rotating disc [13].

### 3 Result and Discussion

#### 3.1 Effect of $\text{Si}_3\text{N}_4$ Reinforcement on the Microstructure of Aluminium Composites

The microstructure of Al–Mg–Zn alloy, as cast and etched surface of squeeze cast aluminium composites of varying weight percentage, are shown in Figs. 3, 4, 5 and 6. It has been observed that the microstructure of synthesized composites shows a dendrite pattern of primary aluminium with grain boundary precipitated eutectic particles. The reinforced particles are uniformly distributed in the matrix alloy without an indication of a cluster. It is also inferred that microstructure confirms streaks of  $\text{Si}_3\text{N}_4$  particles that have occupied the large grain boundary of the primary aluminium grain. These particles occupied the grain boundary

site as they are very fine in structure. However, the addition of a higher percentage of reinforcement shows a higher density of distribution in the metal matrix and hence it appears even in all the fields. The grain boundaries are thicker as the reinforced particles are occupied at the grain boundaries along with the eutectic constituents of the alloy. Due to this the mechanical properties such as strength, stiffness will increase significantly.

The SEM image of synthesized aluminium composites is shown in Fig. 7. The silicon nitride particles are homogeneously distributed through the cross-section and it appears as a granular structure in some regions. It is also inferred that the aluminium matrix composites exhibit a high density of dislocation when ceramic particles reinforced in it. This causes a difference in thermal stress and hence the thermal coefficient of expansion predominantly increased between the matrix and reinforcement particles and this restricts to the motion of dislocation. It is also inferred that as per dispersion strengthening the reinforcement particles are finely dispersed in aluminium alloy matrix and it performs as a barrier to slip of disruption in aluminium alloy matrix are considered to be a significant reason to enhance the mechanical properties of synthesized aluminium composites [14].

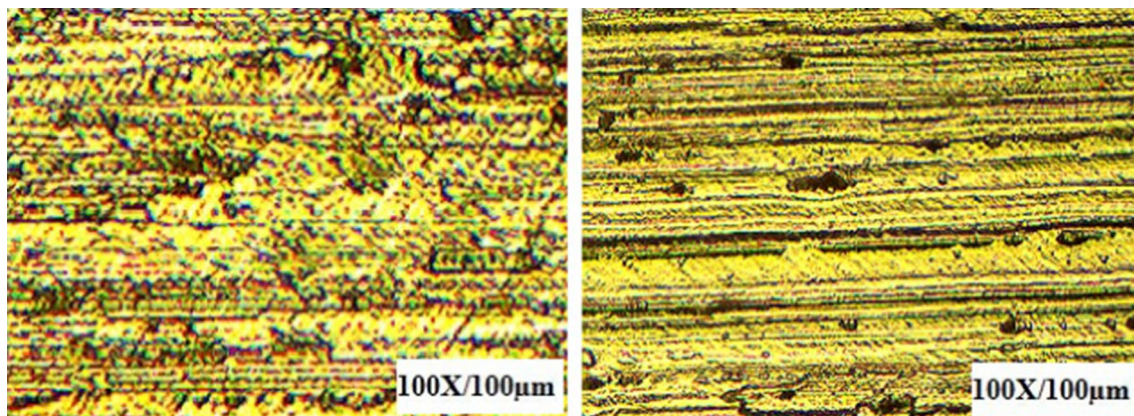


**Fig. 3** Microstructure of Al–Mg–Zn alloy

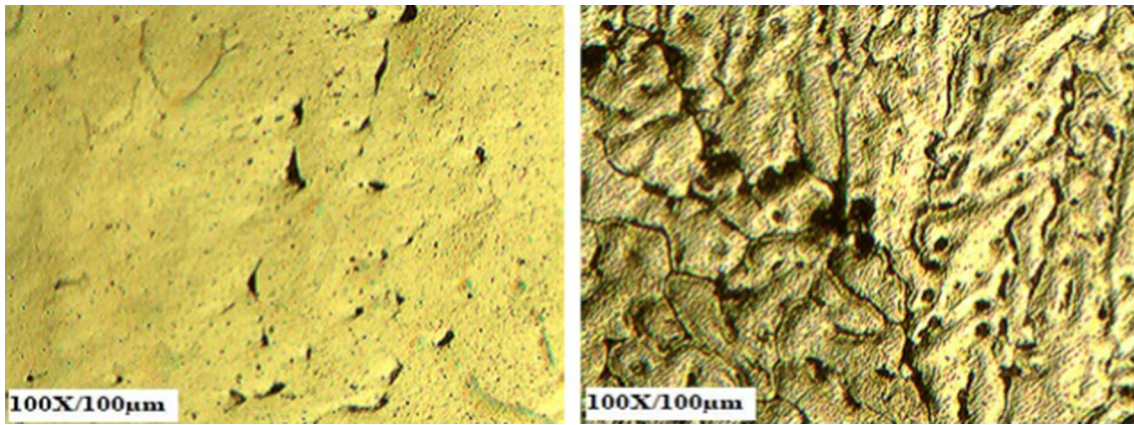


Fig. 4 Microstructure of as cast and etched composites of 3 wt% of Si<sub>3</sub>N<sub>4</sub> reinforced aluminum composites

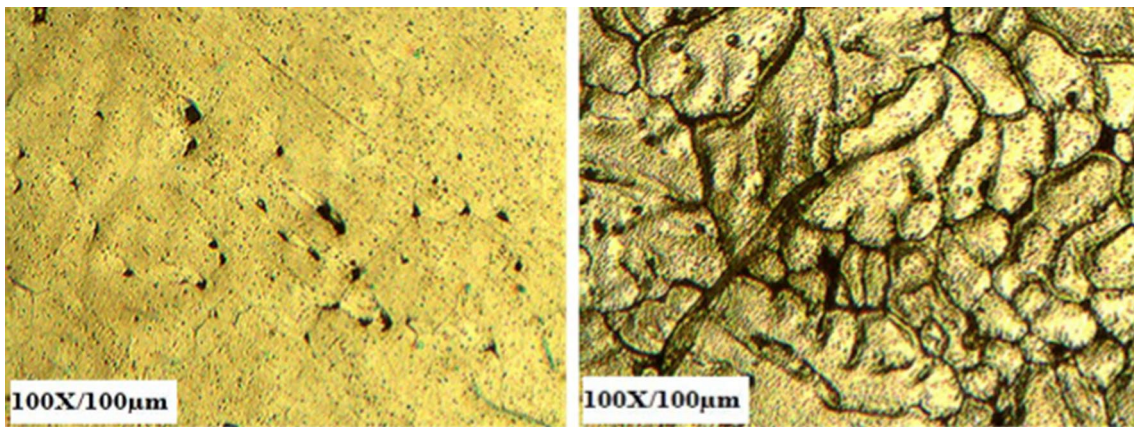


Fig. 5 Microstructure of as cast and etched composites of 6 wt% of Si<sub>3</sub>N<sub>4</sub> reinforced aluminum composites

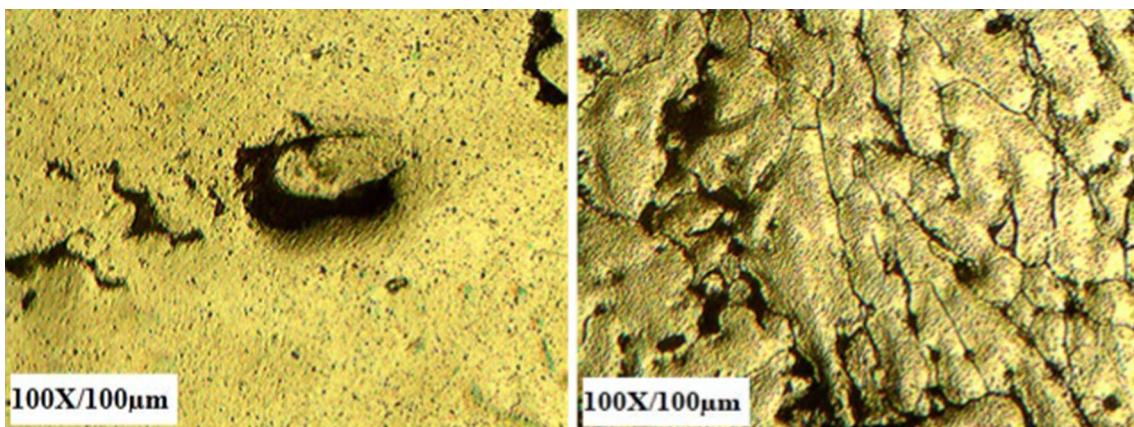
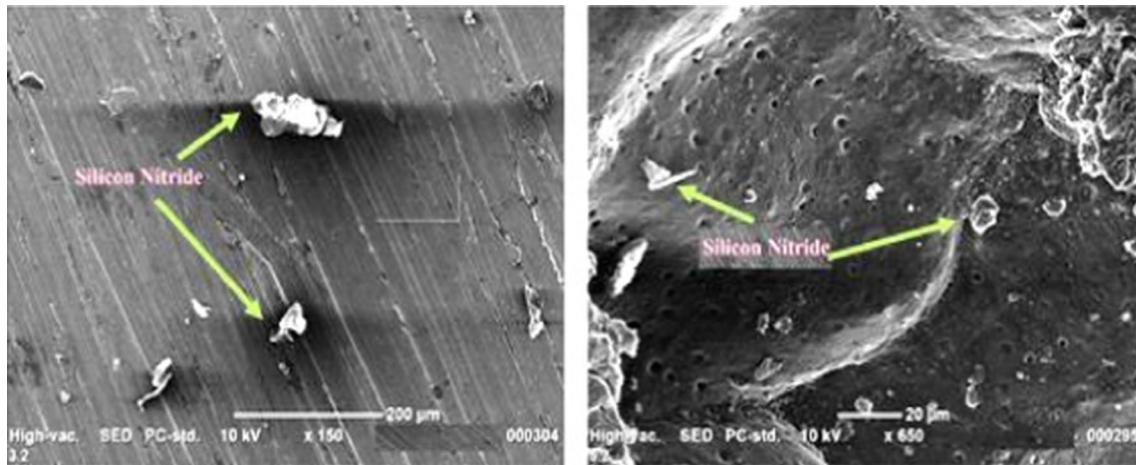


Fig. 6 Microstructure of as-cast and etched composites of 9 wt% of Si<sub>3</sub>N<sub>4</sub> reinforced aluminum composites



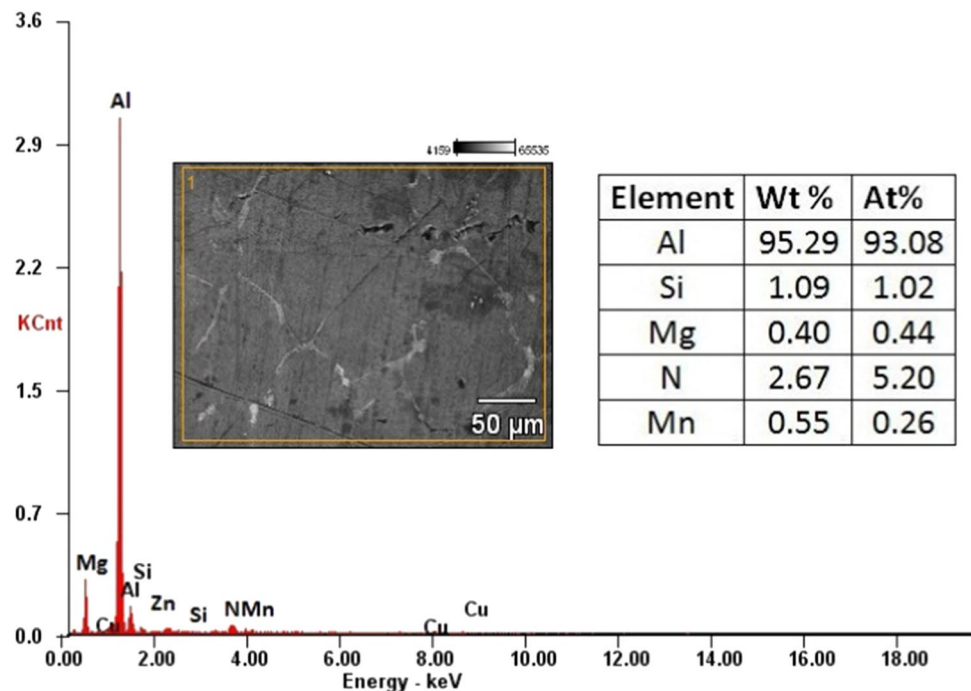
**Fig. 7** SEM image of  $\text{Si}_3\text{N}_4$  reinforced aluminium composites

The concentration of the strengthening particulates in the melt seemed to have lowered the rate of cooling and this induced reduction in the dendritic pattern of solidification. Furthermore the granular metal matrix grains and distribution of  $\text{Si}_3\text{N}_4$  could be inferred. In this context the particle size shows the marginal deformed strengthening particles probably due to heat input. However, the majority of composite particulates have retained the irregular shape and hence the particle size may be varied as incurred in the SEM image. In addition to that the occurrence of  $\text{Si}_3\text{N}_4$  particulates in the aluminium metal matrix is due to the high density of ceramic particulates ( $3.44 \text{ g/cm}^3$ ) as compared

with aluminium ( $2.7 \text{ g/cm}^3$ ), resulting in unreformed  $\text{Si}_3\text{N}_4$  particles at scarce spots indicated as silvery-white in colour which exposed as a rich interface between metal matrix and  $\text{Si}_3\text{N}_4$  particles. The EDAX image of 9 wt% of  $\text{Si}_3\text{N}_4$  reinforced aluminium composites is shown in Fig. 8. It indicates that the developed composites comprehend with a mixture of Al, Si, Mg, N and Mn.

The interfacial reaction plays a significant role in determining the mechanical properties of  $\text{Si}_3\text{N}_4$  reinforced aluminium composites. The inclusion of ceramic particulates interacts with aluminium and it forms another compound which acts as strengthening mechanism to enhance

**Fig. 8** EDAX image of 9%  $\text{Si}_3\text{N}_4$  reinforced aluminium composites



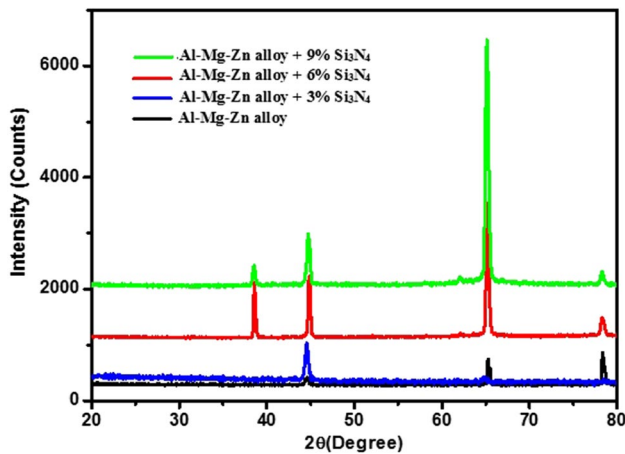


Fig. 9 XRD images of  $\text{Si}_3\text{N}_4$  reinforced aluminium composites

the properties of synthesized composites. This has been inferred in the XRD Fig. 9. However the base materials and strengthening particles can be predicted in the form of dissimilar phase Al–Mg–Zn alloys ( $2\theta = \sim 39^\circ, 45^\circ, 65^\circ$ ),  $\alpha\text{-Si}_3\text{N}_4$  ( $2\theta = \sim 43^\circ, 47^\circ, 48^\circ, 58^\circ, 59^\circ, 78^\circ$ ) and SiC ( $2\theta = \sim 35^\circ, 38^\circ, 60^\circ, 72^\circ$ ) peaks were exposed in XRD as inferred in the literature [15].

### 3.2 Evaluation of Density and Porosity of Synthesized Aluminium Composites

The density and porosity of developed composites are measured as per ASTM E562 & E125 using phase and volume analysis software. It has been observed that the density of developed composites has been increased to a maximum of 1.8% as compared with monolithic aluminium alloy due to the inclusion of  $\text{Si}_3\text{N}_4$  ( $3.44 \text{ g/cm}^3$ ) reinforcement in the matrix alloy. On the other hand, the increment in the the proportion of ceramic particulates amplify the porosity in the fabricated aluminium composites to a maximum of 0.026% for inclusion 9 wt% of  $\text{Si}_3\text{N}_4$ . The higher porosity is due to the entrapment of gases developed during composite processing, and formation of  $\text{SiO}_2$  layer covering the ceramic particulates along with water vapour present during the inception of particulates. As the reinforcing particulates increased, the surface gas layer surrounding the particles were responsible for the floatation of particle clusters and this inhibits the flow of liquid metal [16]. In addition to that, the increase in the porosity of developed composites is due to free energy interface, convection properties and interfacial the reaction between the matrix and reinforcement. It is also inferred that during rapid solidification of molten composites a temperature gradient will occur between the walls of moulds. This is due to the heat transfer coefficient and it tends to change in volume and shrinkage of molten

Table 3 Density and porosity of  $\text{Si}_3\text{N}_4$  reinforced aluminium composites

S. no	Combinations	Density $\text{g/cm}^3$	Porosity(%)
1	Al7075	2.781	–
2	Al7075 + 3% $\text{Si}_3\text{N}_4$	2.810	1.132
3	Al7075 + 6% $\text{Si}_3\text{N}_4$	2.817	1.686
4	Al7075 + 9% $\text{Si}_3\text{N}_4$	2.831	2.326

metal. As a result increases in the percentage of porosity is observed shown in Table 3 [17].

### 3.3 Effect of $\text{Si}_3\text{N}_4$ on Hardness of Aluminium Composites

The hardness of composite is determined by using a micro Vickers hardness test with a load range of 10 grams to 1 kg as shown in Table 4. To achieve accurate hardness value the averages of five readings have been taken out at from each sample of varying weight percentage at different locations. It is inferred that an increased percentage of stronger and stiffer reinforcement and reduction on particle size will significantly increase the hardness of synthesized aluminium composites [18, 19]. On the other hand, wettability, porosity, and interfacial reaction also play a significant role in increasing the hardness of developed composites, since this acts as a bonding strength between the matrix and reinforcement. The hard ceramic reinforcement present in the matrix materials acts as an obstacle and it prevents motion of dislocation. This significantly increases the hardness of silicon nitride composites to a maximum of 43.27% compared with monolithic material.

### 3.4 Influence of $\text{Si}_3\text{N}_4$ Reinforcement on Tensile and Compressive Strength of Aluminium Composites

The tensile strength of synthesized aluminium composites has been characterized as per the ASTM E8 standard using a universal testing machine of maximum load range of 10 ton. The cross head speed is maintained at 0.5 mm/min. It has been observed that the ultimate tensile strength and yield

Table 4 Hardness of  $\text{Si}_3\text{N}_4$  reinforced aluminium composites

S. no	Combinations	Micro-Vickers hardness (HV)
1	Al7075	104.7
2	Al7075 + 3% $\text{Si}_3\text{N}_4$	139.2
3	Al7075 + 6% $\text{Si}_3\text{N}_4$	143
4	Al7075 + 9% $\text{Si}_3\text{N}_4$	149.1

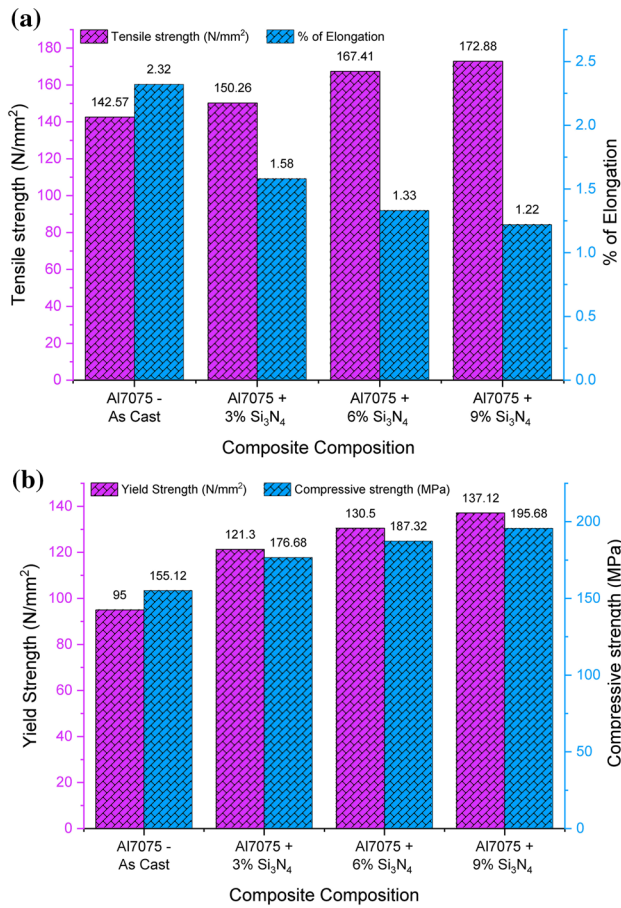


**Fig. 10** a Ultimate tensile strength, % of elongation, b yield strength and compressive strength of Si<sub>3</sub>N<sub>4</sub> reinforced aluminium composites by varying its weight percentage

strength of developed composites have been increased to a maximum of 17.44% and 33.13% respectively compared with monolithic aluminium alloy as shown in Fig. 10a. It is also noted that the load distribution between the matrix and reinforcement is an extreme and hence tensile strength is considerably increased due to the effect of grain refinement as shown in Fig. 11. This restricts the motion of dislocations in the aluminium matrix because of the effect of reinforcement as stated in Orowan mechanism [20]. Moreover, squeeze casting method has been used to develop aluminium composites. It is well known that by using this method the entrapped gas is reduced to the maximum and further grain refinement is achieved. It is also considered to be an essential factor to increase the tensile strength of synthesized aluminium composites.

The percentage elongation of monolithic Al 7075 aluminium alloy and developed aluminium composites of varying weight proportions are compared. It has been noticed that % of elongation minimized to 31.9% in correlation with 3 wt% of Si<sub>3</sub>N<sub>4</sub> reinforced aluminium composites. On

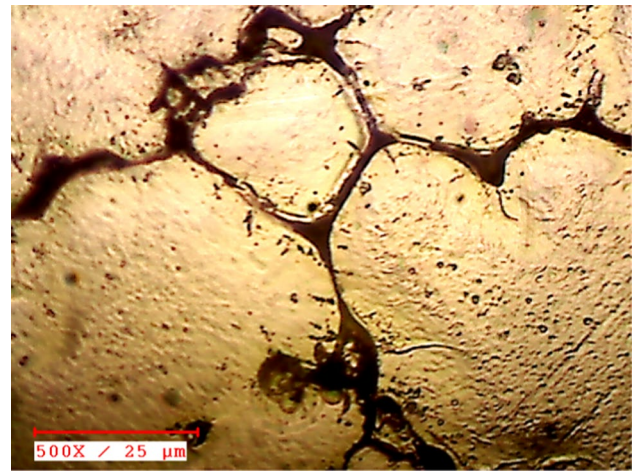


**Fig. 11** Grain refinement of 9 wt% of Si<sub>3</sub>N<sub>4</sub> reinforced aluminium composites

further increasing the proportions of ceramic particulates it is further reduced to 15.82% for 6 wt% and 8.27% of 9 wt% respectively. It is also observed from the experimented composites that the necking is consequently decreased due to increases in the percentage of reinforcement. This is because the increase in the percentage of reinforcement decreases the ductility of synthesized composites and hence brittle nature tends to increase extensively to the characteristic nature of ceramic reinforcement [21]. In this context, the percentage of elongation decreased to a maximum of 47.41% compared with monolithic materials.

The compressive strength of manufactured composites have been evaluated as per ASTM E9 standard at room temperature Fig. 10b. From the observations, it has been inferred that compressive strength increased constantly because of the strong interfacial bonding strength, the dispersion strengthening of strengthening particles between the intermixtures. The uniformly disseminated strengthening particulates in the base material hinders the motion of dislocation in the matrix alloy. This causes a reduction in grain size by increasing particle accumulation in some specified region [22]. It is also observed that by increasing the percentage of reinforcement particles the interface boundaries and the area of interface boundaries between the intermixture increased significantly. Hence, the displacement is piled up at the interface boundaries comparable to the grain boundaries. This proposition combined to causes the high compressive strength of the synthesized composites.

### 3.5 Impact Strength of Si<sub>3</sub>N<sub>4</sub> Reinforced Aluminium Composites

The Impact strength of developed composites has been measured as per ASTM E23 standard using Izod impact



**Table 5** Impact strength of aluminum composites using Si<sub>3</sub>N<sub>4</sub> as reinforcement

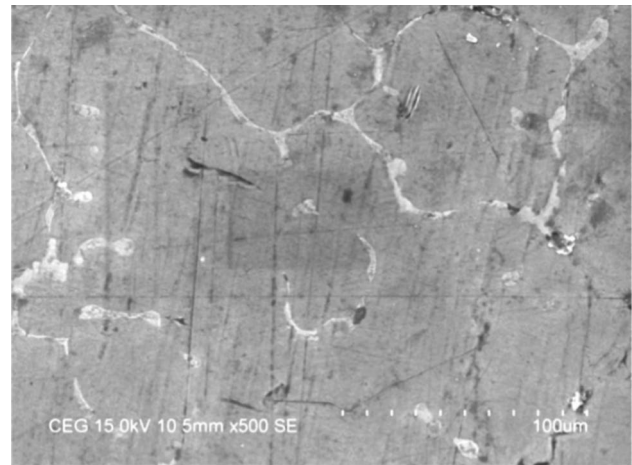
S. no	Combinations	J/m <sup>2</sup>
1	Al7075	1.8
2	Al7075 + 3%Si <sub>3</sub> N <sub>4</sub>	2.2
3	Al7075 + 6%Si <sub>3</sub> N <sub>4</sub>	2.7
4	Al7075 + 9%Si <sub>3</sub> N <sub>4</sub>	4.4

testing machine. It is found that the impact strength of fabricated aluminium composites is enhanced significantly compared with monolithic aluminium alloy as shown in Table 5. This is due to the consequence of the squeeze casting process. By using this process the maximum amount of pores and defects in the synthesized aluminium composites has been reduced to a minimum and hence the grain refinement along with bonding strength of composites has been improved [23]. Subsequently, it results in an increase in ductility and hence the impact strength inherently increased to 144.44% then monolithic aluminium alloy.

### 3.6 Influence of Si<sub>3</sub>N<sub>4</sub> Reinforcement on Corrosion Resistant of Aluminum Composites

The corrosion behavior of particulate reinforced aluminium composites was characterized by various researchers and it was stated that the occurrence of particulate reinforcement particles in the metal matrix cannot enhance its corrosion rate. It significantly depends on size, shape, homogenous distribution of reinforcement, microstructure and interfacial reaction between the matrix and reinforcement [24, 3]. However, a few changes that occur on such factors will affect the corrosion properties of aluminium composites. It is also observed that the inclusion of ceramic reinforcement in the base alloy tends to affect the protective oxide layers of aluminium metal surface. Since they acquire separation in the layer commencement of the corroded surface and it brings forth to the lesser extent of corrosion resistant [25]. However, in the present study, an effort has been to study the corrosion resistant behaviour of aluminium composites using Si<sub>3</sub>N<sub>4</sub> as reinforcement.

The corrosion test of synthesized aluminum composites has been performed as per ASTM B117 salt spray test. It is an intensify type of corrosion and in which the composite samples are subjected to a corrosive environment. The synthesized aluminum composite samples of varying it weight percentage were pre-polished and pre-cleaned before subjecting it into the salt spray chamber for the corrosion test. All the specimens were directed to cleaning with non-aqueous solvent and which is not attacking base aluminium alloy material. The solvent cleaning was done only on the surface of aluminium and care

**Fig. 12** Corrosion resistant of 9% Si<sub>3</sub>N<sub>4</sub> reinforced aluminium composites

is taken to avoid the solvent attack. Then these samples were subjected to salt spray fog corrosion testing chamber.

It is observed that the corrosion rate of the Al7075- Si<sub>3</sub>N<sub>4</sub> (Table 6) decreases with an increasing percentage of strengthening particulates. The better corrosion resistant property is acquired compared with base materials is because of its substantial interfacial mixture, uniformly disseminated Si<sub>3</sub>N<sub>4</sub> in the aluminium matrix, increased in density of distribution, appropriate interfacial bonding of intermixtures acts as a better load bearer when compared with monolithic aluminium 7075 Alloy. It is also inferred that in seawater condition pitting corrosion exhibits due to the presence of NaCl environment. This has been significantly improved and hence the segregation at the grain boundaries also controlled uniform distribution of reinforcement in the matrix alloy as cited in the literature [26, 27]. On the other hand the mechanism of disintegration of silicon nitride in sea water is found in Equ. 1[28].



It is also inferred that the formation of SiO<sub>2</sub> acts as barrier to prevent oxidation in silicon nitride reinforced aluminium composites as shown in Fig. 12. In addition to that the inference of weight loss on each composites has been observed and it has been found that the formation of microcrevices occurs near by the matrix and reinforcement particles interface, deterioration of reinforcement in the aluminium alloy matrix composites [29, 30].

**Table 6** Corrosion resistance of Silicon nitride reinforced aluminium composites

% of Reinforcement	Initial weight (g)	Final weight (g) (After 24 h)	Difference in weight (g)	Corrosion rate (mm/year)
Al7075 + 3% Si <sub>3</sub> N <sub>4</sub>	8.848	8.647	0.201	0.003300838
Al7075 + 6% Si <sub>3</sub> N <sub>4</sub>	8.691	8.524	0.167	0.002792029
Al7075 + 9% Si <sub>3</sub> N <sub>4</sub>	8.782	8.715	0.067	0.001108548

**Table 7** Wear parameters used for characterizing aluminium composites

S.no	% of Composition	Load (N)	Sliding velocity (m/s)	Sliding distance (m)	rpm	Time (S)	Initial weight (g)	Final weight (g)	Wear loss in % (g)
1	Al7075 + 3% Si <sub>3</sub> N <sub>4</sub>	25	1.5	600	955	400	4.496	4.248	5.51601423
2	Al7075 + 3% Si <sub>3</sub> N <sub>4</sub>	35	1.5	600	955	400	4.525	4.334	4.22099447
3	Al7075 + 6% Si <sub>3</sub> N <sub>4</sub>	25	1.5	600	955	400	4.578	4.392	4.78339350
4	Al7075 + 6% Si <sub>3</sub> N <sub>4</sub>	35	1.5	600	955	400	4.486	4.337	3.32144449
5	Al7075 + 9% Si <sub>3</sub> N <sub>4</sub>	25	1.5	600	955	400	4.432	4.220	4.06290956
6	Al7075 + 9% Si <sub>3</sub> N <sub>4</sub>	35	1.5	600	955	400	4.406	4.269	3.10939627

### 3.7 Influence of Reinforcement on Wear Properties of Aluminum Composites

The wear resistance behaviour of the cast composite was evaluated as per the ASTM standard with the following conditions given in Table 7.

Observations were made that the wear loss of fabricated aluminium composites has been significantly decreased by increasing the percentage of Si<sub>3</sub>N<sub>4</sub> strengthening particulates in the aluminium alloy matrix for all the combinations of the applied load. The variation of the friction coefficient ( $\mu$ ) and frictional force (FF) with a varying load of the synthesized composites has been shown in Fig. 13. The friction coefficients reinforced particles are range between 0.06 and 0.16. The applied loads used in the wear test are 25 and 35 N respectively. It is noted that the friction coefficient of the developed composites has been significantly increased. This is due to the strengthening effect of complexes, dislocations in the alloy are ineffective which causes the increase in hardness are the most influential factor to enhance the wear resistance of the manufactured composites. It has been found that during sliding condition thin deep grooves are observed on the worn surface of the composites. This are associated by presence of harder strengthening particulates in the base material. Thus by increasing the proportion of such particulates it exhibits plastic deformation and it results in the formation of grooves. These grooves are coupled with abrasive wear and it is formed while removing the material by the pin and disc during interaction of hard asperities on the surface of a steel disc which wear on the conglomerates. Furthermore the existence of plastic deformation, the

material transfer occurs on the surface of the combinations while sliding induces adhesive wear. It is also found that by applying the same load of 25 N for 6 wt% and 9 wt% of Si<sub>3</sub>N<sub>4</sub> aluminium composite the grooves are found invariable and it restricts plastic deformation of synthesized composites. On the other hand, the load-bearing capacity enhanced continuously.

SEM micrographs of worn surfaces of synthesized composites of varying weight proportions under 35N of applied load are shown in Fig. 14. It is inferred that because of the presence of Si<sub>3</sub>N<sub>4</sub> particulated it restrict the formation of transfer layer between the matrix and reinforcement particles. Due to this effect, fine grooves are constituted on the work surface and hence the wear resistant of synthesized composites significantly increased. It also found no drastic changes occur on the formation of grooves, adhesive wears on applying 35 N on the fabricated composites [31–35].

## 4 Conclusions

In the present study silicon nitride of particle size,  $\leq 10$  microns reinforced with aluminium alloy matrix by varying its weight percentage using squeeze casting has been successfully fabricated and its microstructure and mechanical properties were studied. The conclusions are given below.

1. The microstructure of synthesized aluminium composites is homogeneously distributed throughout its cross-section without indication of the cluster and it confirms

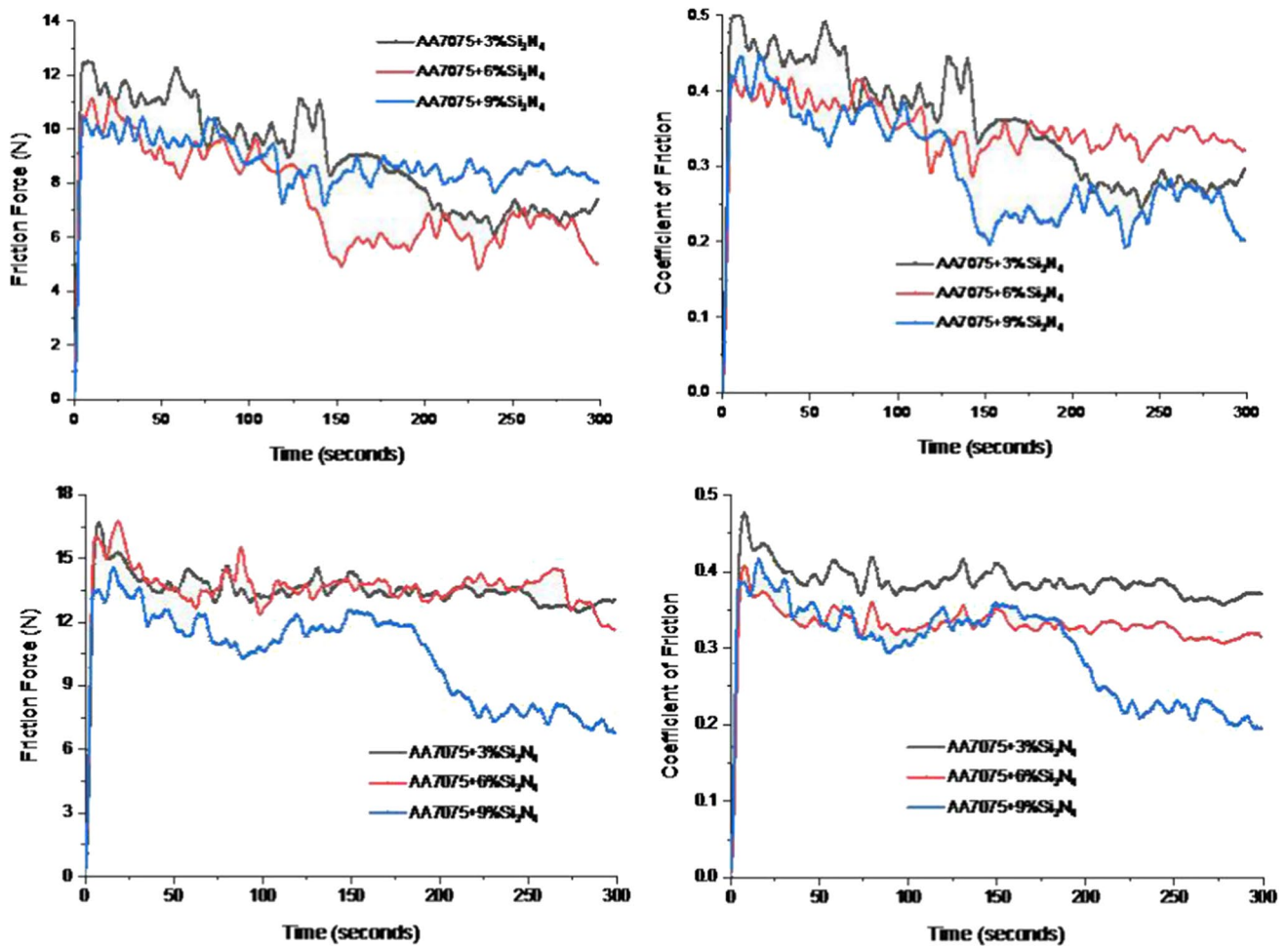


Fig. 13 Frictional force and coefficient of friction of  $\text{Si}_3\text{N}_4$  reinforced aluminium composites by varying load 25 N and 35 N

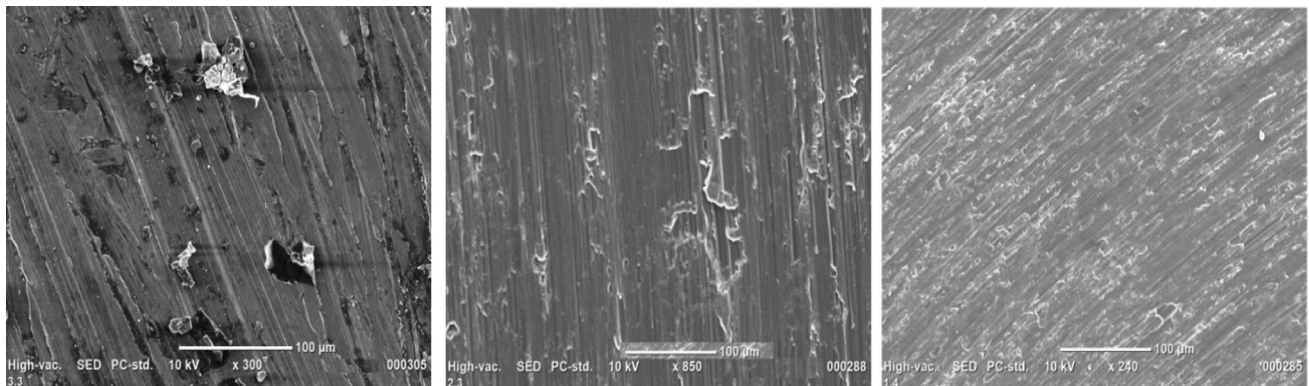


Fig. 14 SEM image of worn surface of  $\text{Si}_3\text{N}_4$  (3 wt%, 6 wt%, and 9 wt%) reinforced aluminium composites for an applied load of 35 N

streaks of  $\text{Si}_3\text{N}_4$  particles that have occupied the large grain boundary of the primary aluminium grain.

2. The inclusion of higher percentage reinforcement in the aluminium matrix alloy increases its, tensile strength

(17.44%), yield strength (3.13%), and decreases the percentage of elongation compared to monolithic aluminium alloy.

3. The hardness (43.27%), compressive strength (25.81%) and impact strength (144%) of the developed composites have been significantly increased due to the inclusion of stiffer and stronger reinforcement in the matrix alloy.
4. The corrosion resistant is considerably enhanced and hence pitting corrosion along with the segregation at the grain boundaries also controlled.
5. The wear rate of aluminium composites is considerably improved due to the effect fine grooves formed on the worn surface.

## References

1. R. Casati, M. Vedani, *Metals* **4**, 65–83 (2014)
2. B.S. Yigezu, M.M. Mahapatra, P.K. Jha, *J. Miner. Mater. Charact. Eng.* **1**, 124–130 (2013)
3. M.O. Bodunrin, K.K. Alaneme, L.H. Chown, *J. Mater. Res. Technol.* **4**, 434–445 (2015)
4. K.A. Kenneth, O.S. Kazeem, *Eng. Sci. Technol. Int. J.* **18**, 416–422 (2015)
5. N. Wang, Z. Wang, G.C. Weatherly, *Metall. Trans. A* **23**, 1423–1430 (1992)
6. T. Matsunaga, J.K. Kim, S. Hardcastle, P.K. Rohatgi, *Tran. Amer. F.* **104**, 1097–1102 (1996)
7. M. Imran, A.R.A. Khan, *J. Mater. Res. Technol.* **8**, 3347–3356 (2019)
8. Z.-Y. Xiu, G.-Q. Chen, G.-H. Wu, W.-S. Yang, Y.-M. Liu, *T. Non-ferr. Metal. Soc.* **21**, s285–s289 (2011)
9. P. Sharma, S. Sharma, D. Khanduja, *J. Asian. Ceram. Soc.* **3**, 352–359 (2015)
10. G.A. Chadwick, T.M. Yue, *Met. Mater.* **5**, 6–12 (1989)
11. G. Anbuhezhiyan, B. Mohan, D. Sathianarayanan, T. Muthuramalingam, *J. Alloy. Compd.* **719**, 125–132 (2017)
12. P. Sharma, S. Sharma, D. Khanduja, *J. Asian Ceram. Soc.* **3**, 352–359 (2015)
13. L.-T. Jiang, G.-H. Wu, W.-S. Yang, Y.-G. Zhao, S.-S. Liu, *T. Non-ferr. Metal. Soc.* **20**, 2124–2128 (2010)
14. C. Kannan, R. Ramanujam, *J. Adv. Res.* **8**, 309–319 (2017)
15. G. Anbuhezhiyan, T. Muthuramalingam, B. Mohan, *Arch. Civ. Mech. Eng.* **18**, 1645–1650 (2018)
16. S.N. Ahmed, J. Hasim, M.I. Ghazali, *J. Compos. Mater.* **39**, 451–466 (2005)
17. D. Priyadarshi, R.K. Sharma, *Mater. Sci. Ind. J.* **14**, 119–129 (2016)
18. A. Kalkanli, S. Yilmaz, *Mater. Design* **29**, 775–780 (2008)
19. S.A. Sajjadi, H.R. Ezatpour, M.T. Parizi, *Mater. Design* **34**, 106–111 (2012)
20. R. Flores-Campos, D.C. Mendoza-Ruiz, P. Amézaga-Madrid, I. Estrada-Guel, M. Miki-Yoshida, J.M. Herrera-Ramirez, R. Martínez-Sánchez, *J. Alloy. Compd.* **495**, 394–398 (2010)
21. K.B. Lee, H.S. Sim, S.Y. Cho, H. Kwon, *Metall. Mater. Trans. A* **32**, 2142–2147 (2001)
22. C. Fenghong, C. Chang, W. Zhenyu, T. Muthuramalingam, G. Anbuhezhiyan, *Silicon* **11**, 2625–2632 (2010)
23. I.B. Deshmanya, G.K. Purohit, *J. Compos. Mater.* **46**, 3247–3253 (2012)
24. S. Thirumalvalavan, N. Senthilkumar, *Indian J. Eng. Mater. S.* **26**, 59–66 (2019)
25. K.K. Alaneme, M.A. Tolulope, A.O. Peter, *J. Mater. Res. Technol.* **3**, 9–16 (2014)
26. G.M. Reddy, P.V. Kumar, K.S. Rao, *Def. Technol.* **11**, 166–173 (2015)
27. F. Toptan, A.C. Alves, I. Kerti, E. Ariza, L.A. Rocha, *Wear* **306**, 27–35 (2013)
28. M. Herrmann, *J. Am. Ceram. Soc.* **96**, 3009–3022 (2013)
29. M. Hermann, J. Schilm, W. Hermel, Michaelis, *J. Ceram. Soc. Jpn.* **114**, 1069–1075 (2006)
30. K. Blugan, G. Daniela, W. Jakob, *Key Eng. Mater.* **368**, 885–887 (2008)
31. P.K. Rohatgi, B.F. Schultz, A. Daoud, W.W. Zhang, *Tribol. Int.* **43**, 455–466 (2010)
32. A. Baradeswaran, A. Elaya Perumal, *Compos. Part B Eng.* **54**, 146–152 (2013)
33. A. Lekatou, A.E. Karantzalis, A. Evangelou, V. Gousia, G. Kaptay, Z. Gacsi, P. Baumli, A. Simon, *Mater. Design* **65**, 1121–1135 (2015)
34. K. Ragupathy, C. Velmurugan, N. Senthilkumar, *J. Balk. Tribol. Assoc.* **24**, 198–217 (2018)
35. V. Selvakumar, S. Muruganandam, N. Senthilkumar, *T. Indian I. Metals* **70**, 1305–1315 (2017)

**Publisher's Note** Springer Nature remains neutral with regard to jurisdictional claims in published maps and institutional affiliations.